Journal of Biomechanics 42 (2009) 1038–1048

Contents lists available at ScienceDirect

Journal of Biomechanics

journal homepage: www.elsevier.com/locate/jbiomech
www.JBiomech.com

Viscoelastic properties of passive skeletal muscle in compression—Cyclic behaviour

M. Van Loocke [a,b,*], C.K. Simms [b], C.G. Lyons [b]

[a] Fluids-Machines Department, Faculté Polytechnique de Mons, Belgium
[b] Centre for Bioengineering, Department of Mechanical and Manufacturing Engineering, Trinity College Dublin, Ireland

ARTICLE INFO

Article history:
Accepted 22 February 2009

Keywords:
Passive skeletal muscle
Viscoelastic properties
Compression
Cyclic tests
Quasi-linear viscoelastic model

ABSTRACT

Skeletal muscle relaxation behaviour in compression has been previously reported, but the anisotropic behaviour at higher loading rates remains poorly understood. In this paper, uniaxial unconfined cyclic compression tests were performed on fresh porcine muscle samples at various fibre orientations to determine muscle viscoelastic behaviour. Mean compression level of 25% was applied and cycles of 2% and 10% amplitude were performed at 0.2–80 Hz. Under cycles of low frequency and amplitude, linear viscoelastic cyclic relaxation was observed. Fibre/cross-fibre results were qualitatively similar, but the cross-fibre direction was stiffer (ratio of 1.2). In higher amplitude tests nonlinear viscoelastic behaviour with a frequency dependent increase in the stress cycles amplitude was found (factor of 4.1 from 0.2 to 80 Hz).

The predictive capability of an anisotropic quasi-linear viscoelastic model previously fitted to stress-relaxation data from similar tissue samples was investigated. Good qualitative results were obtained for low amplitude cycles but differences were observed in the stress cycle amplitudes (errors of 7.5% and 31.8%, respectively, in the fibre/cross-fibre directions). At higher amplitudes significant qualitative and quantitative differences were evident. A nonlinear model formulation was therefore developed which provided a good fit and predictions to high amplitude low frequency cyclic tests performed in the fibre/cross-fibre directions. However, this model gave a poorer fit to high frequency cyclic tests and to relaxation tests. Neither model adequately predicts the stiffness increase observed at frequencies above 5 Hz.

Together with data previously presented, the experimental data presented here provide a unique dataset for validation of future constitutive models for skeletal muscle in compression.

1. Introduction

Finite element models of the human body in compression are used in impact biomechanics, rehabilitation engineering and for simulating surgical procedures (Forbes et al., 2005; Linder-Ganz et al., 2007; Guccione et al., 2001). The models require a good knowledge of the tissue mechanical properties, but the rate dependent three-dimensional compressive behaviour of muscle tissue remains poorly understood.

Skeletal muscle has a fibre-oriented structure consisting of about 80% water, 3% fat and 10% collagenous tissues. It therefore displays anisotropic elasticity as well as time and history dependency. In Van Loocke et al. (2006, 2008), the elastic and viscoelastic properties of passive skeletal muscle were investigated using uniaxial unconfined compression tests performed on fresh porcine muscle tissue *in vitro* and a model was developed to represent the properties observed experimentally. In Van Loocke et al. (2006), quasi-static compression tests at various fibre orientations showed that muscle elastic behaviour is nonlinear and transversely isotropic. In Van Loocke et al. (2008), ramp-and-hold tests at various rates and fibre orientations showed that, above a very small compression rate, the viscoelastic component plays a significant role (approximately 50% of total stress at 0.5 %str s^{-1}). A stiffening effect with compression rate was observed, especially in directions close to the muscle fibres (factor of 5 from 0.05–10 %str s^{-1} in the fibre direction at 30% compression). Skeletal muscle viscoelastic behaviour therefore depends on compression rate and fibre orientation.

In Van Loocke et al. (2006) a transversely isotropic strain dependent Young's moduli (SYM) model was proposed for muscle elasticity. The model yielded excellent fits to the experimental data in the fibre, cross-fibre and 45° directions ($R^2 = 0.99$) up to 30% strain and mean prediction errors for 30° and 60° tests were 3.5% and 9.5%, respectively. In Van Loocke et al. (2008) the model

* Corresponding author at: Fluids-Machines Department, Faculté Polytechnique de Mons, Rue du Joncquois 53, 7000 Mons, Belgium. Tel.: +32 65 374516; fax: +32 65 374513.
E-mail address: melanie.vanloocke@fpms.ac.be (M. Van Loocke).

0021-9290/$ - see front matter © 2009 Elsevier Ltd. All rights reserved.
doi:10.1016/j.jbiomech.2009.02.022

was extended with Prony series to discretise viscoelasticity, which provided a good fit to experimental data in the fibre, cross-fibre and 45° directions at compression rates of 0.5, 1 and 10 %str s^{-1} (errors < 20%). The model also yielded good predictions of muscle behaviour at 0.05 and 5 %str s^{-1} (errors < 25%). However, the predictive capabilities at higher compression rates and during more complex loading were not evaluated.

Muscle compressive properties at very high strain rates (up to 3.7.10^5 %str s^{-1}) have been previously investigated (McElhaney, 1966; Van Sligtenhorst et al., 2006; Song et al., 2007). In the two more recent studies, a split Hopkinson pressure bar apparatus was used. However, the level of control and sensitivity of this apparatus can be questioned.

In this paper, viscoelastic properties of skeletal muscle at strain rates up to 3200 %str s^{-1} are investigated using cyclic loading. Cyclic tests were used instead of airgun/SHPB tests because, despite lower loading rates, cyclic tests allow better control. The predictive capabilities of the quasi-linear viscoelastic (QLV) model (Van Loocke et al., 2008) with parameters based on stress-relaxation tests and a new nonlinear viscoelastic (NLV) model are assessed using these cyclic data. This paper complements the experiments and models in Van Loocke et al. (2006, 2008) which together provide a unique dataset on the mechanical behaviour of skeletal muscle in compression.

2. Materials and methods

2.1. Experimental tests

Uniaxial unconfined compression tests were performed on fresh porcine muscles using the same protocol as in Van Loocke et al. (2008). Muscles were excised from the pelvic limb of male pigs aged 10–12 weeks. From these, cubic samples oriented in the fibre and cross-fibre directions and at 45° and 60° from the fibre direction were cut and kept at room temperature in airtight containers prior to testing, which started within two hours post-mortem. Low and high amplitude cyclic tests were conducted on a Zwick Z005 machine (Zwick GmbH & Co. Ulm, Germany) up to a mean compression level of 25% and saw-tooth cycles of 2% or 10% amplitude were then performed for a duration of 250 s at 0.22 and 0.4 Hz (limited by the Zwick). For higher frequencies, a custom rig was developed (Fig. 1). In this device, samples are compressed between stainless steel platens. Sinusoidal displacements are provided to the bottom platen by an electro-dynamic shaker and various levels of mean compression are achieved by displacement of the top platen. An LVDT measures the displacement of the bottom platen; a static strain gauge load cell on the top platen measures the force; a dynamic load cell (piezoelectric force sensor) is also mounted on the bottom platen to account for inertial effects. Muscle samples were cyclically tested at 5, 20 and 80 Hz. Cycles of 10% amplitude were performed around a mean compression level of 25% for 250 s. Displacement and force signals were acquired using a 16-bit data acquisition card (National Instruments PCI6036E) and Labview. The raw data were digitally low-pass filtered using Matlab (cutoff frequencies of 25, 100 and 400 Hz, respectively, for 5, 20 and 80 Hz tests). Table 1 summarises the tests performed. Six samples were tested in each direction.

2.2. Mathematical modelling

The data obtained were first compared to theoretical predictions from the QLV-SYM model developed in Van Loocke et al. (2008), with parameters derived from fitting to quasi-static and stress-relaxation data (Van Loocke et al., 2006, 2008). See details in the Appendix A.

As shown in the results section, the QLV approach could not fully capture the nonlinear behaviour observed for muscle tissue during high amplitude cyclic tests. Therefore, the generalisation by Poon and Ahmad (1998) of Schapery's nonlinear viscoelastic approach (Schapery 1969) was adopted

$$\sigma_{ij}(t) = h_e\left[\sum_k\sum_l G^{\infty}_{ijkl}\varepsilon_{kl}\right] + h_1\int_0^t \sum_k\sum_l \left[\Delta G_{ijkl}(\xi_{ijkl} - \xi'_{ijkl})\frac{d}{d\tau}(h_2\varepsilon_{kl})\right] d\tau \quad (1)$$

where G^{∞}_{ijkl} and ΔG_{ijkl} represent, respectively, the equilibrium and transient components of the relaxation modulus. The scalar functions h_e, h_1, h_2 depend on the strain tensor and the reduced time is influenced by the mechanical strain via

$$\xi_{ijkl} = \int_0^t \frac{dt}{a_{\tau ijkl}(E(t'))} \quad (2)$$

This NLV model was adapted to include the SYM formulation for the elastic behaviour of muscle tissue—the SYM formulation taking the role of h_e and h_2 in Eq. (1). The terms h_l and a_τ were then introduced to account for viscoelastic nonlinearities (h_l and a_τ are, respectively, denoted h_j and a_j in the following

Fig. 1. Custom built high speed cyclic testing rig. (A) Top platen; (B) bottom platen; (C) LVDT transducer; (D) static load cell; (E) dynamic load cell; and (F) connection with shaker.

Table 1
Summary of cyclic tests performed on porcine skeletal muscle.

Type of test	Cycles amplitude (%)	Frequency (Hz)	Compression rate (%str s^{-1})	Test direction
Low amplitude, low frequency	2	0.22	1	F, XF
High amplitude, low frequency	10	0.22 and 0.4	5 and 10	F, 45°, 60°, XF
High amplitude, high frequency	10	5, 20 and 80	200, 800 and 3200	F, 45°, 60°, XF

equations). The Cauchy stress in direction j can therefore be expressed as

$$\sigma_j(t) = \sigma_j^e G_j(t) + h_j(\tilde{\varepsilon}_j) \int_0^t G_j(\xi_j - \xi'_j) \frac{\partial \sigma_j^e[\tilde{\varepsilon}_j(\tau)]}{\partial \tau} d\tau \quad (3)$$

with

$$\xi_j = \int_0^t \frac{dt'}{a_j[\tilde{\varepsilon}_j(t')]} \quad (4)$$

h_j and a_j were chosen as

$$h_j(\tilde{\varepsilon}_j) = h_{1j}\tilde{\varepsilon}_j + h_{2j}\tilde{\varepsilon}_j^2$$
$$a_j(\tilde{\varepsilon}_j) = 1 - a_{1j}\tilde{\varepsilon}_j + a_{2j}\tilde{\varepsilon}_j^2 \quad (5)$$

A Prony series expansion is adopted for the reduced relaxation function, $G_j(t) = p_{\infty j} + \sum_{i=1}^{N} p_{ij} \exp(-t/\tau_{ij})$ and the SYM formulation is introduced for the elastic stress, $\sigma_j^e = \sigma_{\infty j}/p_{\infty j} = k_{1j}\tilde{\varepsilon}_j + k_{2j}\tilde{\varepsilon}_j^2 + k_{3j}\tilde{\varepsilon}_j^3/p_{\infty j}$.

This leads to

$$\sigma_j(t) = p_{\infty j}\sigma_j^e(t) + h_j(\tilde{\varepsilon}_j) \sum_{i=1}^{N} \int_0^t p_{ij} \exp\left(\frac{-(\xi_j - \xi'_j)}{\tau_{ij}}\right) \frac{\partial \sigma_j^e[\tilde{\varepsilon}_j(\tau)]}{\partial \tau} d\tau \quad (6)$$

The recursive method of Poon and Ahmad (1998) to perform the time integration was implemented in Matlab and the parameters were fitted using the Matlab function *lsqnonlin*.

3. Results

3.1. Low amplitude, low frequency tests

Fig. 2 presents results of 2% amplitude, 0.22 Hz saw-tooth cyclic tests for the fibre and cross-fibre directions (compression rate of 1 %str s^{-1}). Fig. 2(b) illustrates the cyclic stress relaxation of the tissue, with peak/valley stresses decreasing over time.

Fig. 3 compares experimental and theoretical results obtained with the QLV-SYM model for these tests. The model provides a good qualitative prediction of muscle cyclic-relaxation behaviour. The overall relaxation and phase corresponds very well but the

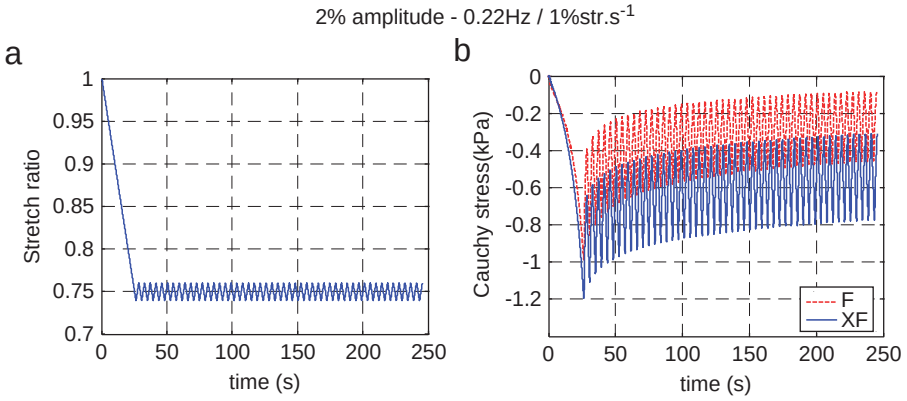

Fig. 2. (a) Deformation history applied to porcine samples during 2% amplitude cyclic compression tests performed at 0.22 Hz (1 %str s^{-1}) and (b) corresponding cyclic stress-relaxation curves obtained in fibre and cross-fibre directions.

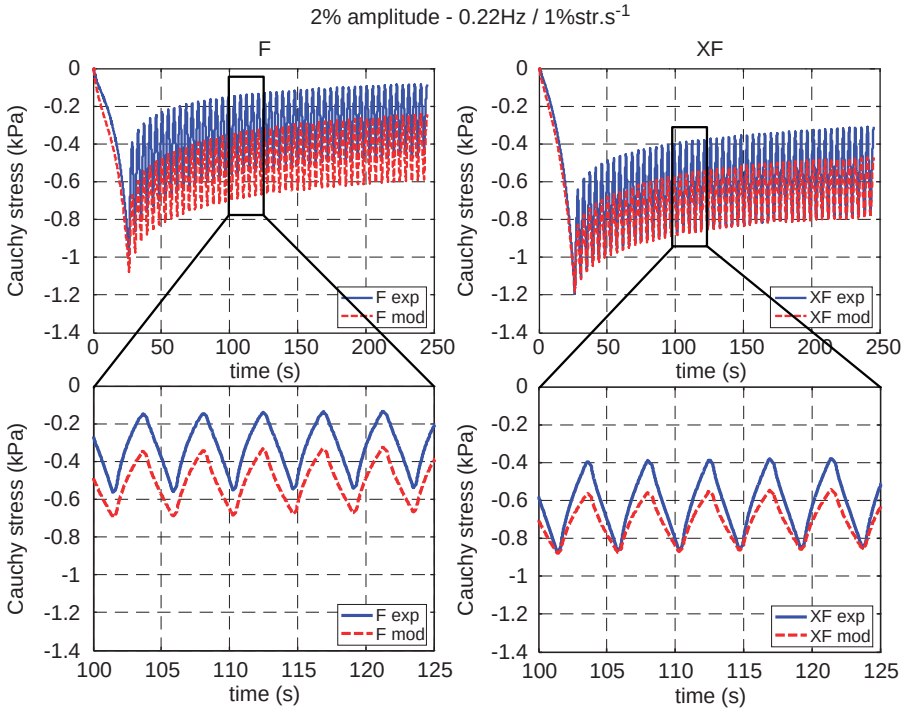

Fig. 3. Comparison between experimental results (▬) and QLV-SYM model predictions (▬) for low amplitude cyclic compression tests performed in (left) fibre and (right) cross-fibre directions at 0.22 Hz. The bottom graphs represent a close-up view of the results (black box area).

predictions under-estimate the stress amplitude of the cycles by 7.5% in the fibre direction and 31.8% in the cross-fibre direction. Nonetheless, the predictive capability of the model is good since the model parameters are derived from ramp-and-hold stress-relaxation tests.

3.2. High amplitude, low frequency tests

This section presents results from 10% amplitude, 0.22 and 0.4 Hz (5 and 10 %str s^{-1}) cyclic tests. Fig. 4 shows that results obtained in the fibre direction are qualitatively similar at both frequencies, the main difference being the peak stress reached after the ramp and the amplitude of the stress cycles (ratio of 1.28). Cyclic stress relaxation is observed, but valley stresses relax quicker than the peaks: within each cycle, the deformation amplitude is sufficient to reduce the stress close to zero, even though a mean compression level of 20% remains.

Fig. 5 presents stress–time curves at 0.4 Hz (a) for the ramp and first few cycles and (b) following relaxation. After the ramp at 10 %str s^{-1}, the fibre direction is the stiffest, followed by the cross-fibre results, while the 45° and 60° results are almost identical. However, after cyclic relaxation, the fibre and cross-fibre results are nearly identical but the 45° direction is the least stiff; showing more stress relaxation has occurred in the fibre and 45° directions. These results are compared to higher frequency results in Fig. 10.

Fig. 6 compares experimental and theoretical results obtained with the QLV-SYM model for 10% amplitude, 0.4 Hz cyclic tests. Graphs (c) and (d) show that the model predicts muscle behaviour

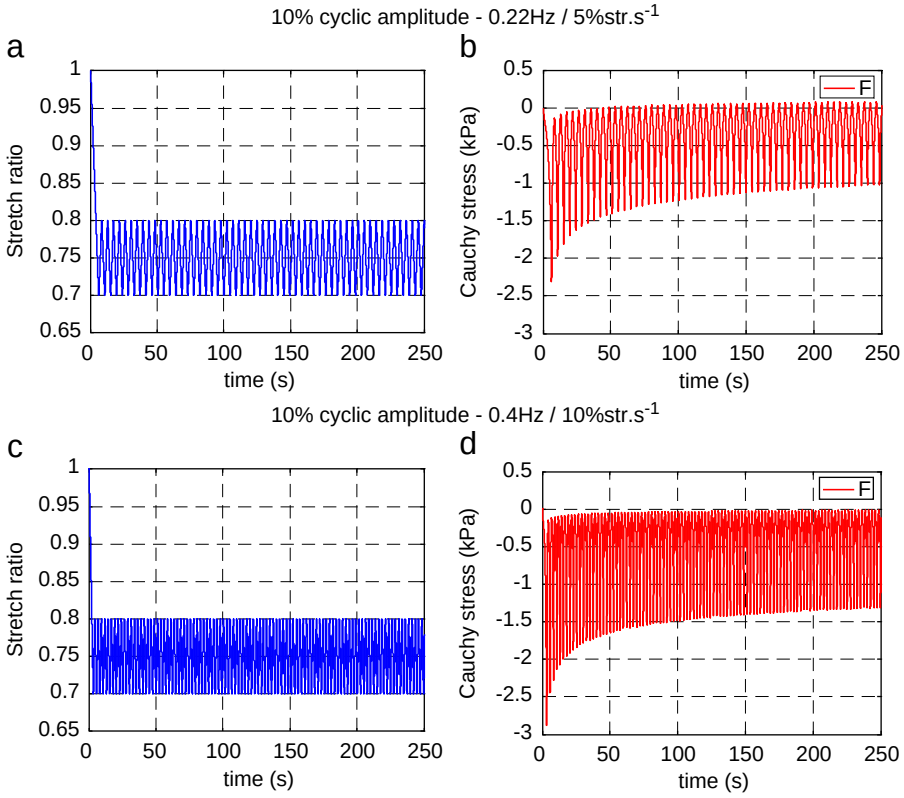

Fig. 4. (a) and (c) Deformation history applied to fresh porcine samples during high amplitude cyclic compression tests performed respectively at 0.22 and 0.4 Hz (5 and 10 %str s^{-1}). (b) and (d) Corresponding cyclic stress-relaxation curves obtained in fibre direction.

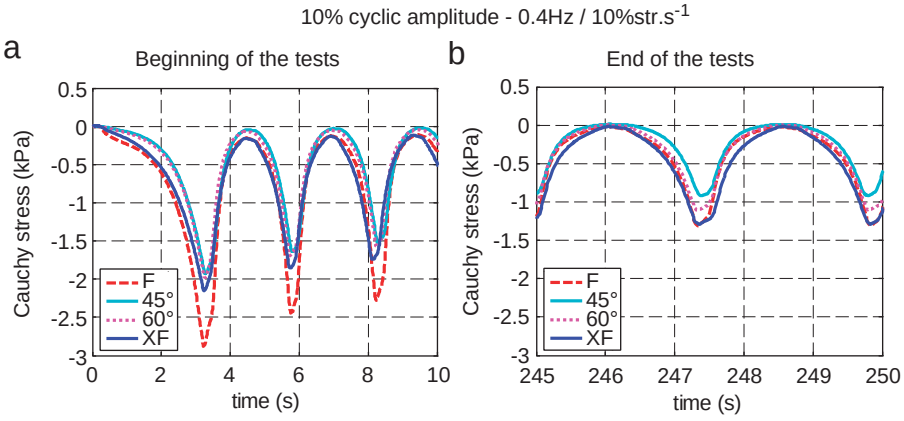

Fig. 5. Close-up comparing stress–time curves at various orientations of the muscle fibres for high amplitude, low frequency cyclic tests.

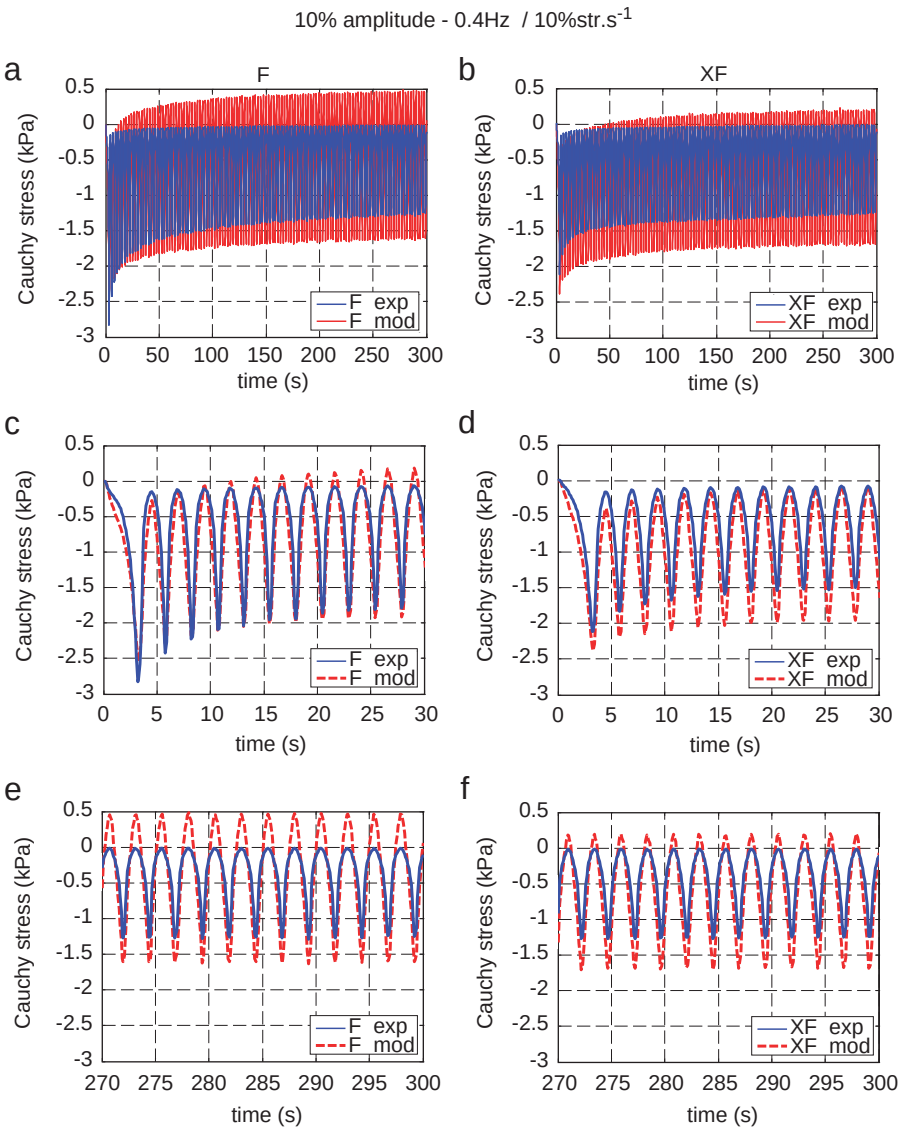

Fig. 6. Comparison between experimental results (—) and QLV-SYM model predictions (—) for high amplitude cyclic compression tests performed in (left) fibre and (right) cross-fibre directions at 0.4 Hz (10 %str s^{-1}). The bottom graphs represent a close-up view of the results (c and d) at the beginning and (e and f) at the end of the tests.

for the ramp and the first few cycles relatively well (cycle stress amplitude for the first 5 cycles under-estimated by 3% in the fibre direction and over-estimated by 16% in the cross-fibre direction). However, the difference between prediction and experiment increases when the number of cycles increases (cycle stress amplitude for the last 5 cycles over-estimated by 65% in the fibre direction and 52% in the cross-fibre direction). The model predicts similar relaxation behaviour during loading and unloading leading to cycles of constant amplitude; faster and smaller relaxation was however observed experimentally for the unloading stress.

These differences are more significant in the fibre than the cross-fibre direction because a higher peak stress and a greater amount of cyclic stress relaxation are observed experimentally in the latter.

The NLV-SYM model was then fitted to these data (10% amplitude, 0.4 Hz). Fig. 7 shows that the model provides a good fit to the experimental data ($R^2 = 0.98$ in the fibre direction; $R^2 = 0.99$ in the cross-fibre direction) and captures the nonlinear behaviour in the cyclic tests except for discrepancies during the ramp phase due to the multiplication of the viscoelastic terms by a second order polynomial (h_j in Eq. (6)). Table 2 presents parameters values.

3.3. High amplitude, high frequency tests

This section presents results from high amplitude cyclic tests performed on the custom rig at 5, 20 and 80 Hz (200, 800 and 3200 %str s^{-1}). Fig. 8 presents results of tests performed in the fibre direction; similar results are obtained at 5, 20 and 80 Hz, the main difference being the amplitude reached by the stress cycles. Fig. 9 presents a close-up view of stress–time curves at the beginning and at the end of the tests. As before, more stress relaxation occurs in the fibre and 45° directions. Just after the compressive ramp, the fibre direction is the stiffest. However, after relaxation all directions are nearly identical. Fig. 10 shows the influence of frequency on the stress cycle amplitude obtained during 10% amplitude cyclic tests (frequency range 0.22–80 Hz). At each frequency, the amplitude of the stress cycle is similar in all orientations. At higher frequencies, the anisotropy is reduced after cyclic relaxation. For each orientation, the amplitude of the stress

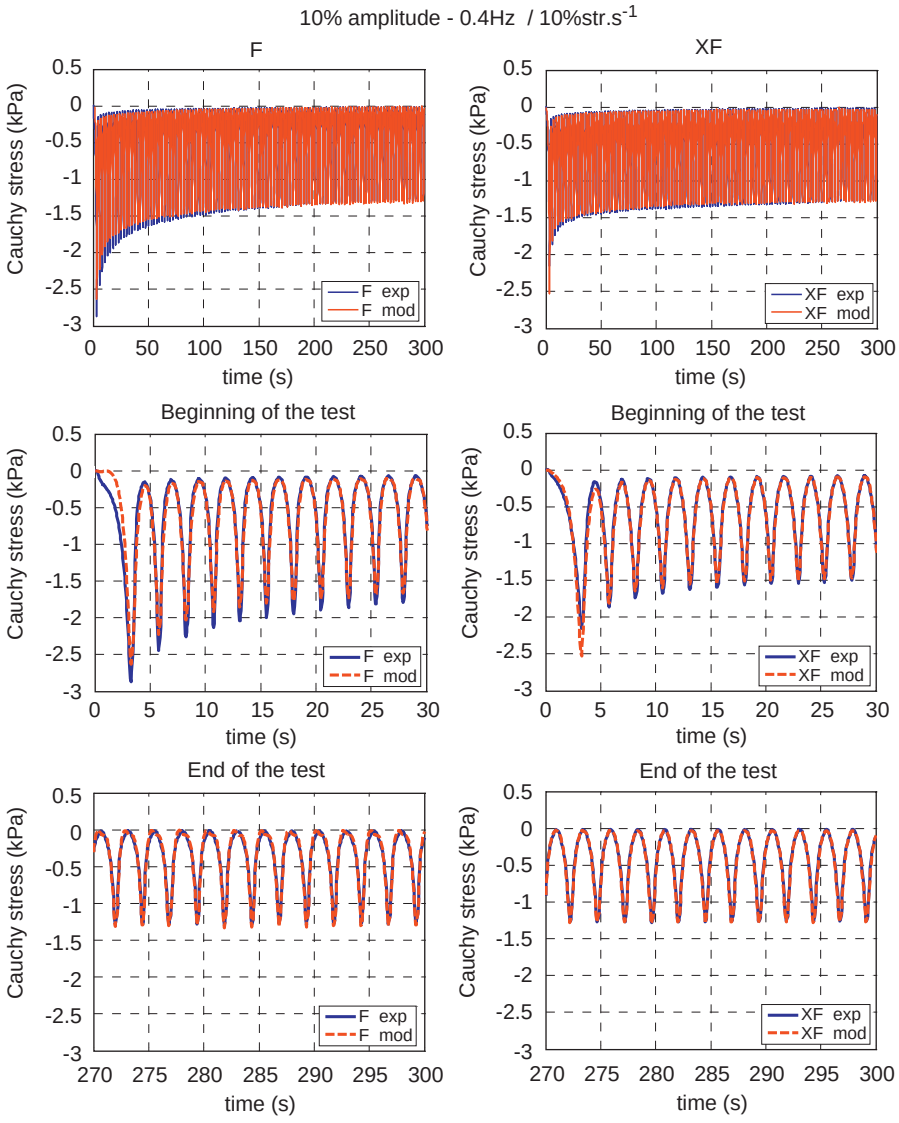

Fig. 7. Comparison between experimental results (—) and NLV-SYM model fitting (—) for high amplitude cyclic compression tests performed in fibre (left) and cross-fibre (right) directions at 0.4 Hz.

Table 2
Parameters for the NLV-SYM model fitted to high amplitude cyclic data obtained at 0.4 Hz on fresh porcine muscle tissue in fibre (left) and cross-fibre (right) directions.

F					XF				
k_{1L} (kPa)	k_{2L} (kPa)	k_{3L} (kPa)	–	–	k_{1T} (kPa)	k_{2T} (kPa)	k_{3T} (kPa)	–	–
1.005	2.989	10.985			1.293	0.911	10.869		
p_{1L}	p_{2L}	p_{3L}	p_{4L}	p_{5L}	p_{1T}	p_{2T}	p_{3T}	p_{4T}	p_{5T}
0.374	0.285	0.077	0.078	0.101	0.097	0.532	0.072	0.000	0.086
τ_{1L} (s)	τ_{2L} (s)	τ_{3L} (s)	τ_{4L} (s)	τ_{5L} (s)	τ_{1T} (s)	τ_{2T} (s)	τ_{3T} (s)	τ_{4T} (s)	τ_{5T} (s)
0.6	6	30	60	300	0.6	6	30	60	300
h_{1L}	h_{2L}	a_{1L}	a_{2L}	–	h_{1T}	h_{2T}	a_{1T}	a_{2T}	–
2.337	12.532	2.337	12.532	–	0.858	9.771	0.858	9.771	–

cycle increases substantially with frequency (approximately fivefold from 0.22 to 80 Hz).

Figs. 11 and 12 compare experimental and theoretical results obtained with the QLV-SYM model for 10% amplitude cyclic tests performed at 5 and 20 Hz in the fibre and cross-fibre directions.

The stress cycle amplitude increases with frequency for muscle tissue and higher peak stresses are reached in the fibre than in the cross-fibre direction after the compressive ramp. Fig. 11 shows that the model predicts results obtained in the cross-fibre direction at 5 Hz relatively well. However, in the fibre direction the peak stress observed experimentally is not reached. Fig. 12 shows similar results for the tests performed at 20 Hz in both directions: the model does not predict the increase in stiffness observed experimentally with frequency. In fact, nearly identical

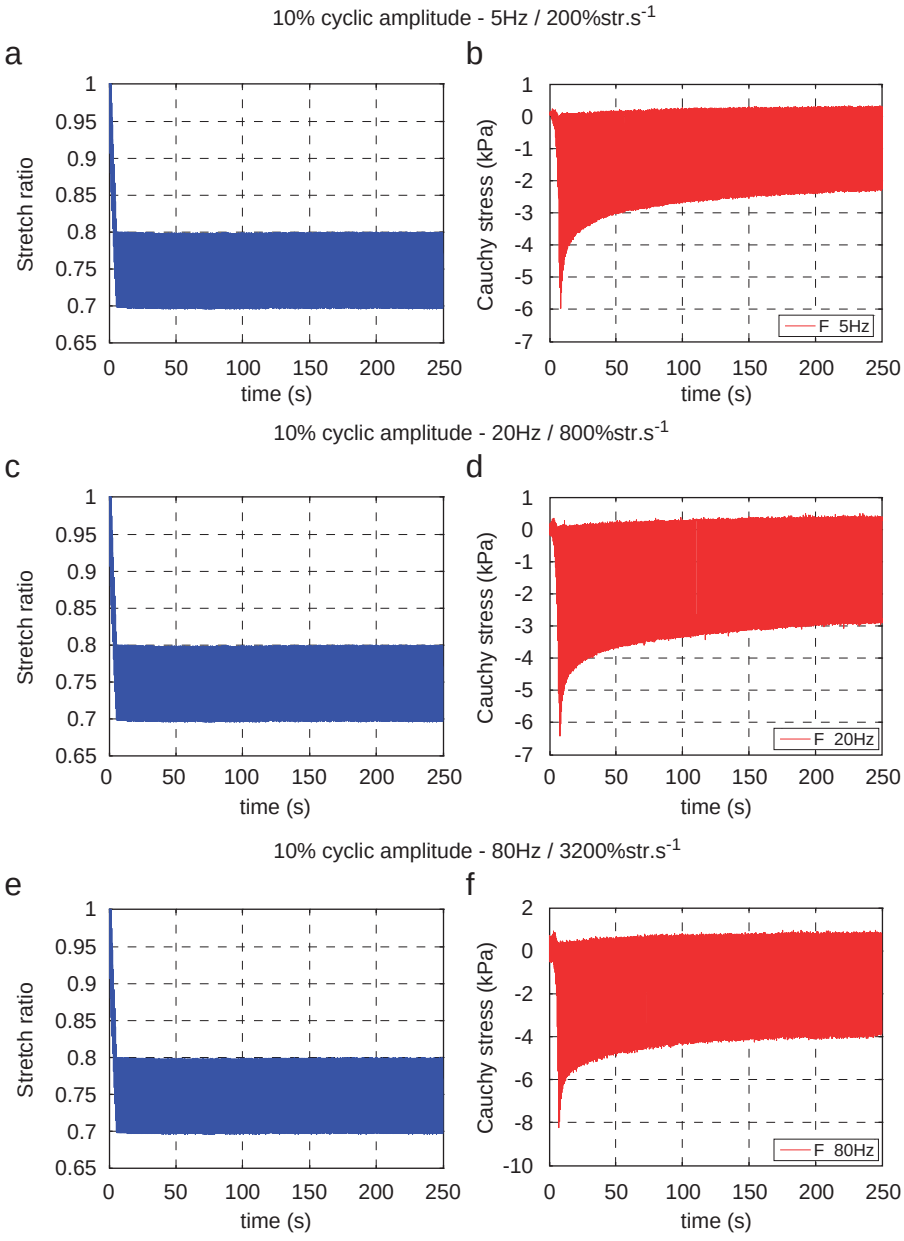

Fig. 8. (a), (c), (f) Deformation history applied to fresh porcine samples during high amplitude cyclic compression tests performed, respectively, at 5, 20 and 80 Hz (200, 800 and 3200 %str s^{-1}). (b), (d), (f) Corresponding cyclic stress-relaxation curves obtained in fibre direction.

stress amplitudes are obtained with the model at 5, 20 and 80 Hz because the maximum value of stress that can be predicted by the model has been reached, as will be elaborated in the discussion. At these frequencies, the NLV-SYM model also fails to sufficiently predict the increase in stiffness observed with frequency.

3.4. *Stress-relaxation tests—NLV-SYM model predictions*

Using the parameters derived from cyclic tests (Table 2), the NLV-SYM model was then used to predict muscle relaxation behaviour. Fig. 13 shows that the response is not as good as previously obtained with the QLV-SYM model (Van Loocke et al., 2008). Although theoretical and experimental results remain close, the model relaxes faster than muscle tissue and under-predicts the peak stresses reached after compression due to the influence of the nonlinear term a_j, which reduces the value of the relaxation constants at higher compression levels. Fig. 14 compares the percentage errors obtained between experimental and theoretical peak stresses for the QLV-SYM and the NLV-SYM models. Peak stress errors remain below 17% at all rates with the quasi-linear model but reach 32.8% with the nonlinear model at a compression rate of 0.5 %str s^{-1}.

4. Discussion

In this paper, passive skeletal muscle behaviour under cyclic compressive loading at various frequencies was investigated and the predictive capabilities of two model formulations were tested. Tests were performed on fresh porcine muscle samples with cycles of 2% or 10% amplitude and frequencies ranging from 0.22 to 80 Hz (5 to 3200 %str s^{-1}). In 2% amplitude, 0.22 Hz tests, linear viscoelastic behaviour was observed. Qualitatively, fibre and cross-fibre results were similar, though the cross-fibre direction is stiffer than the fibre direction (ratio of 1.2). However, during 10%

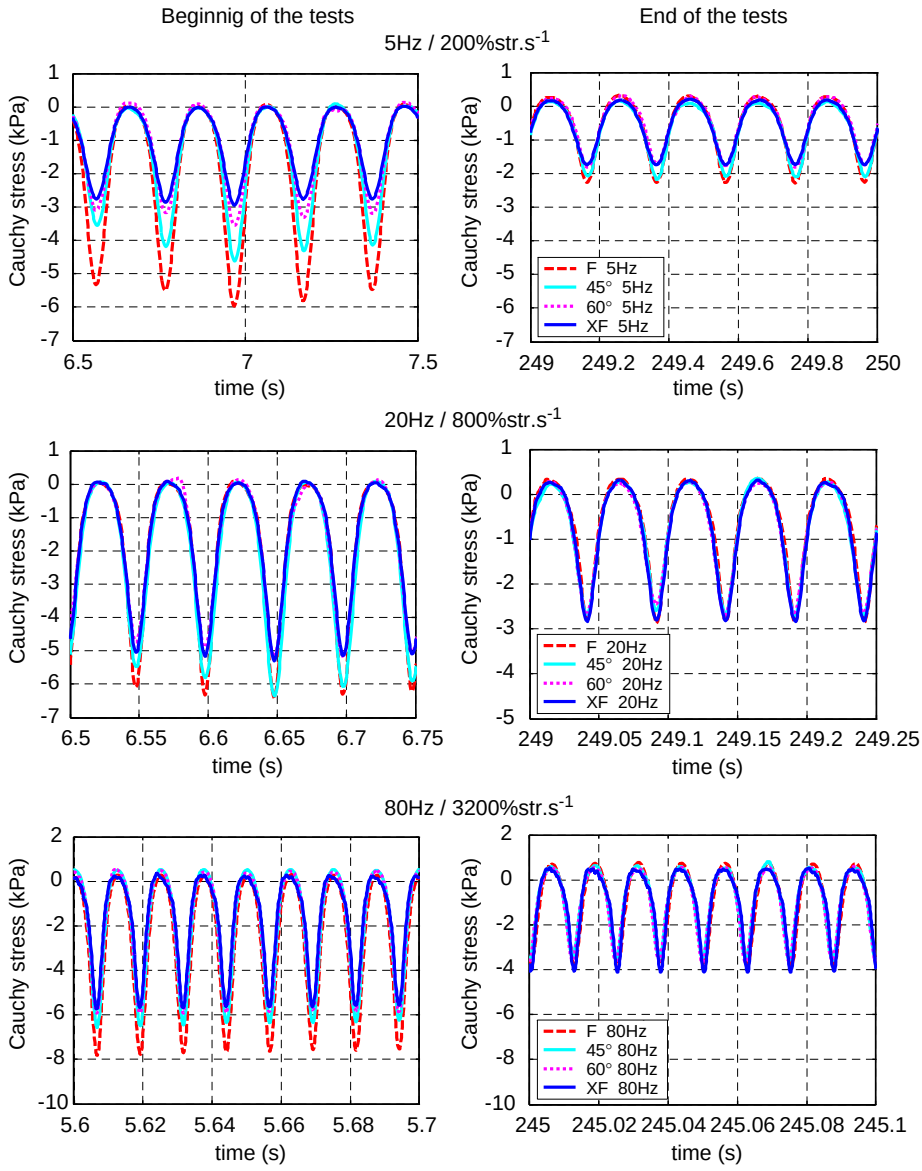

Fig. 9. Close-up comparing stress–time curves at various orientations of the muscle fibres for high amplitude, high frequency cyclic tests.

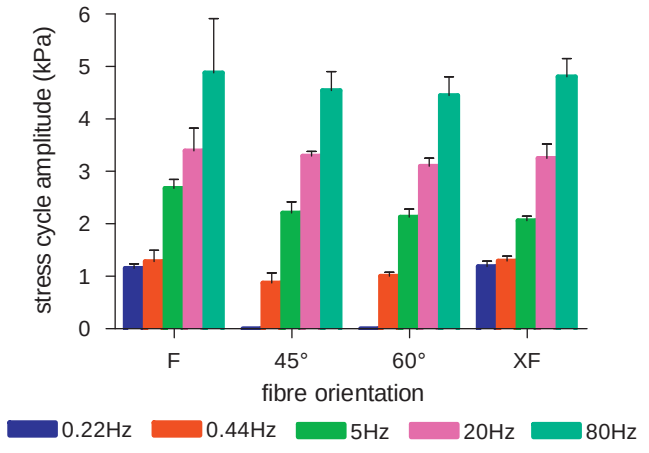

Fig. 10. Evolution with frequency of the stress cycle amplitude for 10% amplitude cyclic tests performed on fresh porcine muscle samples.

amplitude tests the tissue displayed nonlinear viscoelastic behaviour: peak stresses decreased gradually with an increasing number of cycles but valley stresses appeared completely relaxed after only a small number of cycles (stress variation <0.03 kPa after 20 cycles). During these tests, a greater amount of stress relaxation was observed in directions closer to the muscle fibres. This confirms results obtained in Van Loocke et al. (2008), the viscoelastic component has a greater influence in directions closer to the muscle fibres. For 10% amplitude tests performed at 5–80 Hz similar results were found, though the amplitude of the stress cycles increased with frequency (approximately fivefold from 0.22 to 80 Hz).

Overall good predictions were obtained with the QLV-SYM model (Van Loocke et al., 2008) concerning stress relaxation and low amplitude cyclic tests at lower frequencies. For higher amplitude cycles the model presented poorer predictive capabilities due to nonlinearities in the tissue response. Nonlinearities were therefore introduced in the model by means of two additional strain-dependent terms (a_j and h_j in Eq. (5)). This NLV-SYM model provided a good fit to the low frequency cyclic

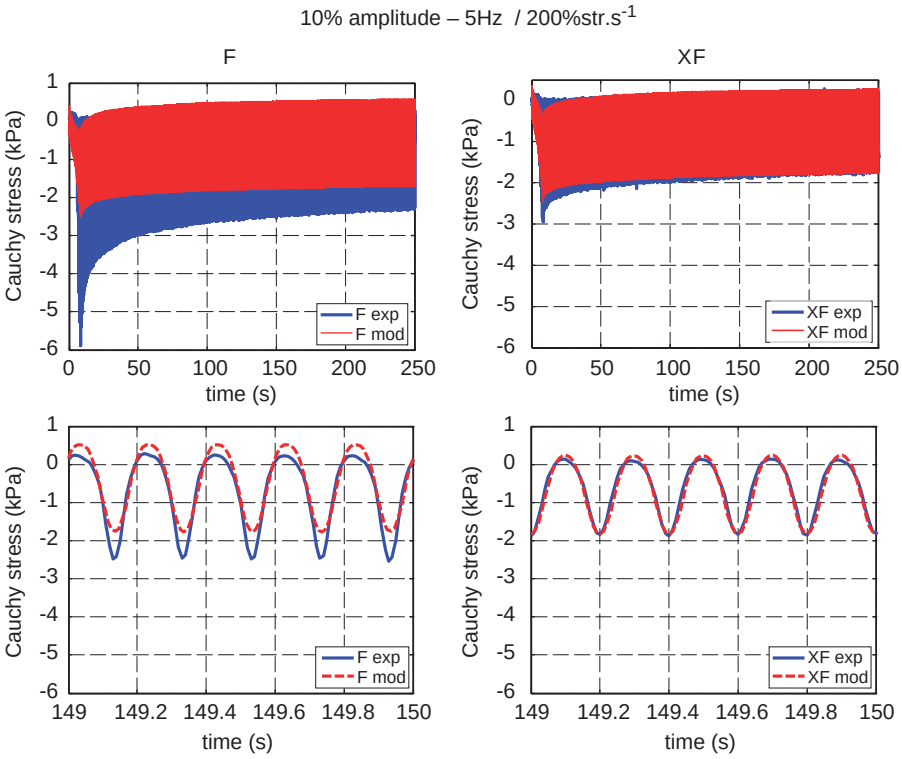

Fig. 11. Comparison between experimental results (▬) and QLV-SYM model predictions (▬) for high amplitude cyclic compression tests performed in (left) fibre and (right) cross-fibre directions at 5 Hz. The bottom graphs represent a close-up view of the results around 150 s.

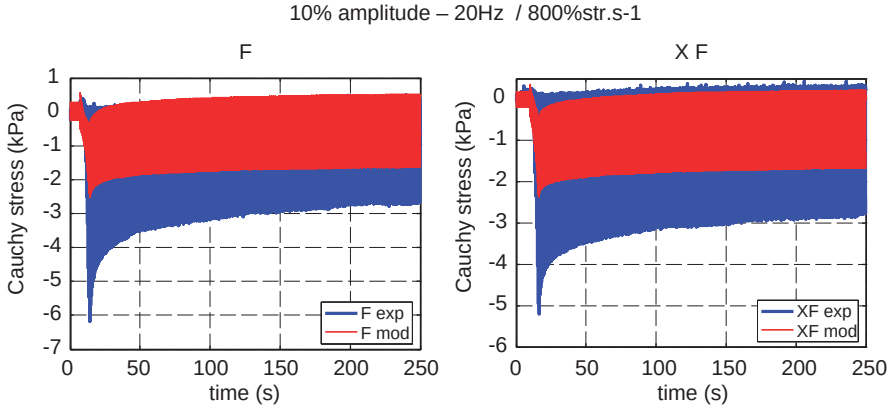

Fig. 12. Comparison between experimental results (▬) and QLV-SYM model predictions (▬) for high amplitude cyclic compression tests performed in (left) fibre and (right) cross-fibre directions at 20 Hz.

experimental data and is able to capture the nonlinear behaviour observed during low frequency, high amplitude cyclic tests.

A direct comparison of these results with the literature is difficult given the lack of published data. McElhaney (1966) used an airgun-type testing machine to test the dynamic response of bovine muscle tissue up to 75% compression and rates ranging from 0.1 to 10^5 %str s^{-1}. The influence of anisotropy and rigor mortis were not addressed. Van Sligtenhorst et al. (2006) used a SHPB apparatus to measure the compressive properties of bovine muscle tissue up to 80% compression and rates ranging from 1 to $2.3.10^5$ %str s^{-1} in the fibre direction. McElhaney reported that the maximum compressive stress at 75% strain is multiplied by only 2.6 from 0.1 to 10^5 %str s^{-1}. Van Sligtenhorst et al. (2006) observed a multiplication factor of 4.5 between 10^5 and $2.3.10^5$ %str s^{-1} at 30% compression. In Van Loocke et al. (2008) a similar ratio of 5 was observed between the stress reached (at 30% compression) at 0.05 and 10 %str s^{-1}. In the present paper, the amplitude of the stress cycle is multiplied by 4.1 from 5 to 3200 %str s^{-1}. Strain levels above 30% were not tested to minimise the possible influence of fluid expulsion in isolated tissue samples.

Song et al. (2007) also performed *in vitro* compression tests on porcine muscle tissue at rates ranging from 0.7 to $3.7.10^5$ %str s^{-1}. The very high strain rates considered and the presentation of the data does not allow a direct comparison with the present data. Song et al. (2007) concluded that porcine muscle compressive response is nonlinear and strongly strain-rate sensitive, but their results show that data obtained at 0.7 and 7 %str s^{-1} are identical and the strain-rate effect remains small below $5.4.10^4$ %str s^{-1}. This contradicts the findings by Grieve and Armstrong (1988) as well as the data obtained in this paper and questions the sensitivity of the SHPB apparatus. Overall, the studies published qualitatively confirm the results in this paper, i.e. skeletal muscle

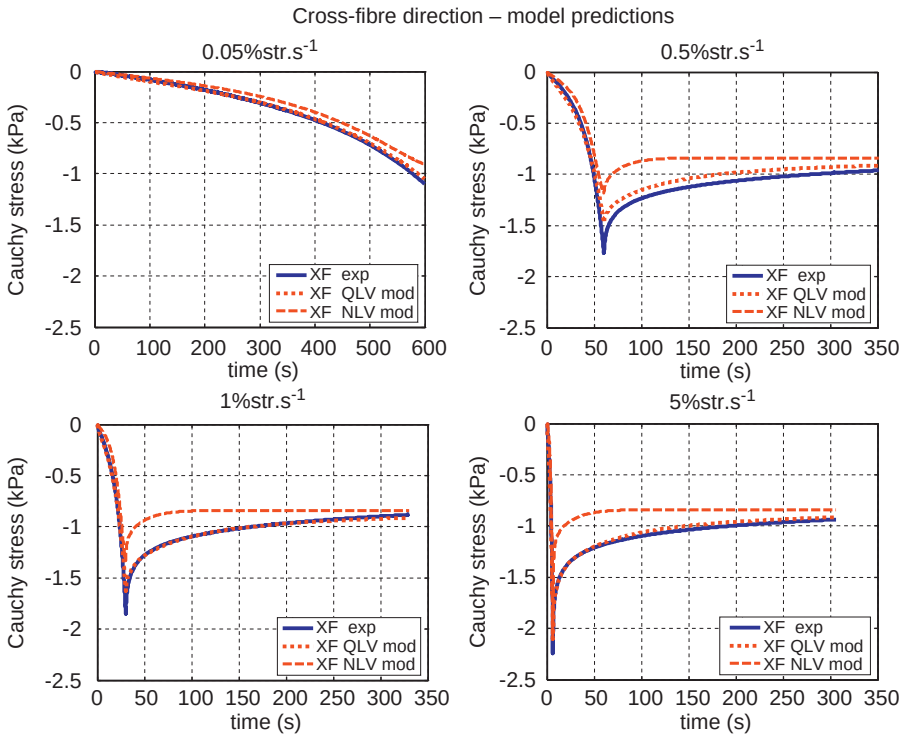

Fig. 13. Comparison between experimental stress-relaxation results, QLV-SYM and NLV-SYM models predictions in the cross-fibre direction.

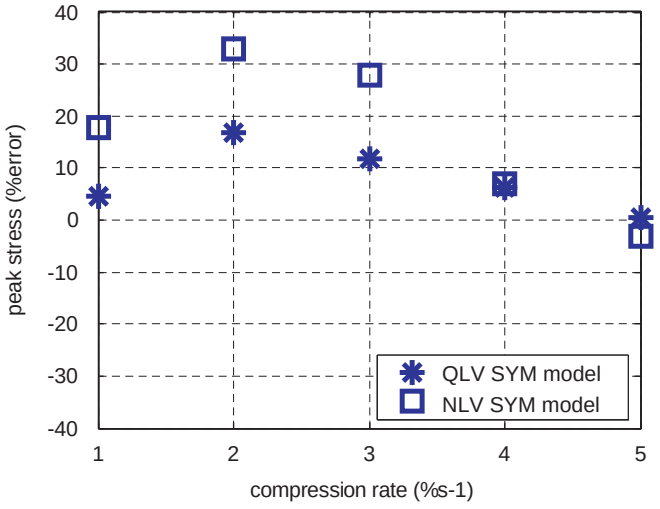

Fig. 14. Percentage errors between experimental and theoretical peak stresses in cross-fibre direction for the QLV-SYM model and the NLV-SYM model.

compressive properties depend on deformation rate, but quantitative comparisons are difficult due to differences in the experimental protocols used.

At higher strain rates, both viscoelastic models proposed cannot predict the increase in stiffness observed because the maximum predicted stress is $\sigma_j^e = (k_{1j}\tilde{\varepsilon}_j + k_{2j}\tilde{\varepsilon}_j^2 + k_{3j}\tilde{\varepsilon}_j^3)/(1 - \sum_{i=1}^{n} p_{ij})$. This is the instantaneous elastic stress for a step input. However, the stress at 10 %str s^{-1} already approaches this maximum, and this limitation was previously noted in modelling ligament viscoelasticity (Pioletti et al., 1998; Woo et al., 1981). Pioletti and Rakotomanana (2000) proposed a model in which stress relaxation and strain-rate effects are discriminated according to the time scale of their effects. The addition of such a term in the models proposed here will therefore be a focus of future research.

The experimental data and the model presented here are directly suitable for applications in surgical simulation and rehabilitation engineering, and a finite element implementation of the models is in progress. The applicability of the experimental data for impact biomechanics applications can be assessed by the following order of magnitude comparison: in a 48 km/h unrestrained frontal vehicle impact, assuming the occupant's body strikes the vehicle interior at 48 km/h, the tissue compression rate is 13.33 m/s. For a midbody region muscle thickness of 5 cm, this represents a compression rate of 26660 %str s^{-1} and the highest compression rate of 3200 %str s^{-1} presented in this paper is about 8 times lower than this. This shows that, although higher strain-rate data are still required, the cyclic tissue tests presented here are close to the relevant loading rates in medium severity impact biomechanics applications. Furthermore, the testing rates performed range from 0.05 to 3200 %str s^{-1}, or a factor of 64,000. Vibration problems currently limit higher testing rates with the present apparatus, but future work should make it possible to provide data at significantly higher loading rates.

5. Conclusions

The experimental data presented in this paper, together with previous work (Van Loocke et al., 2006, 2008) provide a unique dataset for skeletal muscle elastic and viscoelastic properties under compressive ramp-and-hold and cyclic loading. Strain-dependent stiffening and linear viscoelasticity were observed for low amplitude low frequency cyclic tests, but nonlinear behaviour was observed in high amplitude and high frequency cyclic testing. Quasi-linear and nonlinear viscoelastic models with good predictive capabilities for specific loading conditions have been proposed, though neither model can predict all of the tissue behaviour observed experimentally. These models are directly suitable for finite element implementation in surgical simulation and rehabilitation engineering applications, and future work with

a similar approach should yield muscle compression data appropriate for automotive impact biomechanics applications.

The experimental data obtained in this study will be made freely available.

Conflict of interest statement

We, the undersigned state that there are no conflicts of interest in this paper titled: Viscoelastic properties of passive skeletal muscle in compression—Cyclic behaviour.

Acknowledgements

This project is funded by the Programme for Research in Third Level Institutions (PRTLI), administered by the Irish Higher Education Authority (HEA).

Appendix A. Supplementary data

Supplementary data associated with this article can be found in the online version at doi:10.1016/j.jbiomech.2008.10.038.

References

Forbes, P.A., Cronin, D.S., Deng, Y.C., Boismenu, M., 2005. Numerical human model to predict side impact thoracic trauma. In: Gilchrist, M.D. (Ed.), IUTAM Symposium on Impact Biomechanics: From Fundamental Insights to Applications. Springer, pp. 441–450.

Guccione, J.M., Moonly, S.M., Wallace, A.W., Ratcliffe, M.B., 2001. Residual stress produced by ventricular volume reduction surgery has little effect on ventricular function and mechanics: a finite element model study. Journal of Thoracic and Cardiovascular Surgery 122, 592–599.

Grieve, A.P., Armstrong, C.G., 1988. Compressive properties of soft tissues. In: de Groot, G., Hollander, A.P., Huijing, P.A., van Ingen Schenau, G.J. (Eds.), Biomechanics XI-A. International series on biomechanics. Free University Press, Amsterdam, pp. 531–536.

Linder-Ganz, E., Shabshin, N., Itzchak, Y., Gefen, A., 2007. Assessment of mechanical conditions in sub-dermal tissues during sitting: A combined experimental-MRI and finite element approach. Journal of Biomechanics 40, 1443–1454.

McElhaney, J.H., 1966. Dynamic response of bone and muscle tissue. Journal of Applied Physiology 21, 1231–1236.

Pioletti, D.P., Rakotomanana, L.R., Benvenuti, J.F., Leyvraz, P.F., 1998. Viscoelastic constitutive law in large deformations: application to human knee ligaments and tendons. Journal of Biomechanics 31, 753–757.

Pioletti, D.P., Rakotomanana, L.R., 2000. Non-linear laws for soft biological tissues. European Journal of Mechanics A/Solids 19, 749–759.

Poon, H., Ahmad, M.F., 1998. A material point time integration procedure for anisotropic, thermo rheologically simple, viscoelastic solids. Computational Mechanics 21, 236–242.

Schapery, R.A., 1969. On the characterization of nonlinear viscoelastic materials. Polymer Engineering and Science 9, 295–310.

Song, B., Chen, W., Weerasooriya, T., 2007. Dynamic and quasi-static compressive response of porcine muscle. Journal of Biomechanics 40 (13), 2999–3005.

Van Loocke, M., Lyons, C.G., Simms, C.K., 2006. A validated model of passive muscle in compression. Journal of Biomechanics 39 (16), 2999–3009.

Van Loocke, M., Lyons, C.G., Simms, C.K., 2008. Viscoelastic properties of passive skeletal muscle in compression. Stress-relaxation behaviour and mathematical modelling. Journal of Biomechanics 41, 1555–1566.

Van Sligtenhorst, C., Cronin, D.S., Wayne Brodland, G., 2006. High strain rate compressive properties of bovine muscle tissue determined using a split Hopkinson bar apparatus. Journal of Biomechanics 39, 1852–1858.

Woo, S.L., Gomez, M.A., Akeson, W.H., 1981. The time and history-dependent viscoelastic properties of the canine medical collateral ligament. Journal of Biomechanical Engineering 103, 293–298.